Ore Geology Reviews 141 (2022) 104598

Contents lists available at ScienceDirect

Ore Geology Reviews

journal homepage: www.elsevier.com/locate/oregeorev

Two significant quartz-wolframite-veining mineralization events in the Jiangnan Orogen, South China: Constraints from *in-situ* U–Pb dating of wolframite in the Dongping and Dahutang W-(Cu-Mo) deposits

Shiwen Yang [a,b], Fasheng Lou [a], Chang Xu [c], Chengyou Feng [d], Shenghua Cao [a], Deru Xu [b,*], Yanwen Tang [e,*]

[a] Geological Survey of Jiangxi Province, Nanchang 330030, Jiangxi, China
[b] School of Earth Sciences, East China University of Technology, Nanchang 330013, Jiangxi, China
[c] School of Earth Sciences, China University of Geosciences (Wuhan), Wuhan 430074, Hubei, China
[d] Institute of Mineral Resources, Chinese Academy of Geological Sciences, Beijing 100037, China
[e] State Key Laboratory of Ore Deposit Geochemistry, Institute of Geochemistry, Chinese Academy of Sciences, Guiyang 550081, Guizhou, China

ARTICLE INFO

Keywords:
Jiangnan tungsten (W) metallogenic belt
Wolframite *in-situ* U–Pb dating
Dongping and Dahutang W deposits
Quartz-vein type wolframite

ABSTRACT

The Jiangnan Orogen of South China is a world-class tungsten (W) metallogenic belt. Although the ore-forming ages of porphyry-skarn scheelite deposits in the Jiangnan Orogen are well quantified, the timing of quartz-vein type wolframite deposition is still ambiguous. Two typical quartz-vein type wolframite deposits, the Dongping and Dahutang deposits, were chosen for analysis. For the Dongping W deposit, a lower intercept $^{206}Pb/^{238}U$ age of 129.5 ± 5.4 Ma (1σ, MSWD = 0.75) was obtained for wolframite, which agrees well with the zircon weighted average mean $^{206}Pb/^{238}U$ age of 129.8 ± 0.3 Ma (2σ, MSWD = 0.4) from samples of the three granite units (biotite granite, muscovite granite and two-mica granite of the hidden pluton). This indicates that the quartz-wolframite-vein mineralization in the Dongping deposit has a genetic relationship with the hidden Dongping pluton. The wolframite samples from the Dahutang W deposit yielded a lower intercept $^{206}Pb/^{238}U$ age of 137.3 ± 4.8 Ma (1σ, MSWD = 1.9), which corresponds to previously reported scheelite Sm–Nd, molybdenite Re–Os and muscovite ^{40}Ar–^{39}Ar ages from the Dahutang deposit (142–138 Ma), as well as to monazite and zircon U–Pb ages for the ore-related biotite granite, biotite granite porphyry and granite porphyry (143–138 Ma). In combination with previous studies, these results constrain two significant quartz-wolframite veining events at ~130 Ma and ~140 Ma in the Jiangnan W metallogenic belt.

1. Introduction

The Jiangnan tungsten (W) metallogenic belt (JNWB), which is located in the eastern segment of the Jiangnan Orogen, South China (Xu et al., 2017), is a newly identified world-class porphyry–skarn W belt, and has a total WO_3 resource of more than 6 Mt (Fig. 1a, b; Mao et al., 2017; Mao et al., 2019; Mao et al., 2020; Wu et al., 2019a; Wu et al., 2019b; Wu et al., 2020). The major porphyry W deposits are Yangchuling (Mao et al., 2017), Dahutang (Feng et al., 2012; Jiang et al., 2015), Dongyuan (Qin et al., 2010; Wu et al., 2019a; Zhou et al., 2011) and Matou (Zhao et al., 2015), while the skarn W deposits are known as Zhuxi (Chen et al., 2015), Xianglushan (Dai et al., 2018; Feng et al., 2018; Zhang et al., 2008), Xiaoyao (Su et al., 2018), Dawujian (Li et al., 2015), Jitoushan (Song et al., 2012), Zhuxiling (Kong et al., 2018) and Gaojiaba (Fig. 1b; Xiao et al., 2017). Tungsten mineralization in the JNWB predominantly occurs as porphyry-skarn scheelite developed at the proximal contacts of granite plutons which were formed during the Jurassic to Cretaceous (Mao et al., 2020). However, wolframite mineralization is likely abundant in the JNWB, such as the discovered Dongping W deposit, which consists of quartz-vein type wolframite (Li et al., 2016; Yang et al., 2020b). In addition, quartz-vein type wolframite ores are also present in some porphyry and skarn scheelite deposits, such as Dahutang, Shangjinshan and Dawujian (Feng et al., 2012; Jiang et al., 2015; Li et al., 2015; Tang et al., 2019). Thus it can be seen that quartz-vein type wolframite is a very important W mineralization style in the JNWB. However, previous studies have yielded no constraints on the

* Corresponding authors.
E-mail addresses: xuderu@ecut.edu.cn (D. Xu), tyw_xt@126.com (Y. Tang).

https://doi.org/10.1016/j.oregeorev.2021.104598
Received 25 May 2021; Received in revised form 13 November 2021; Accepted 21 November 2021
Available online 29 November 2021

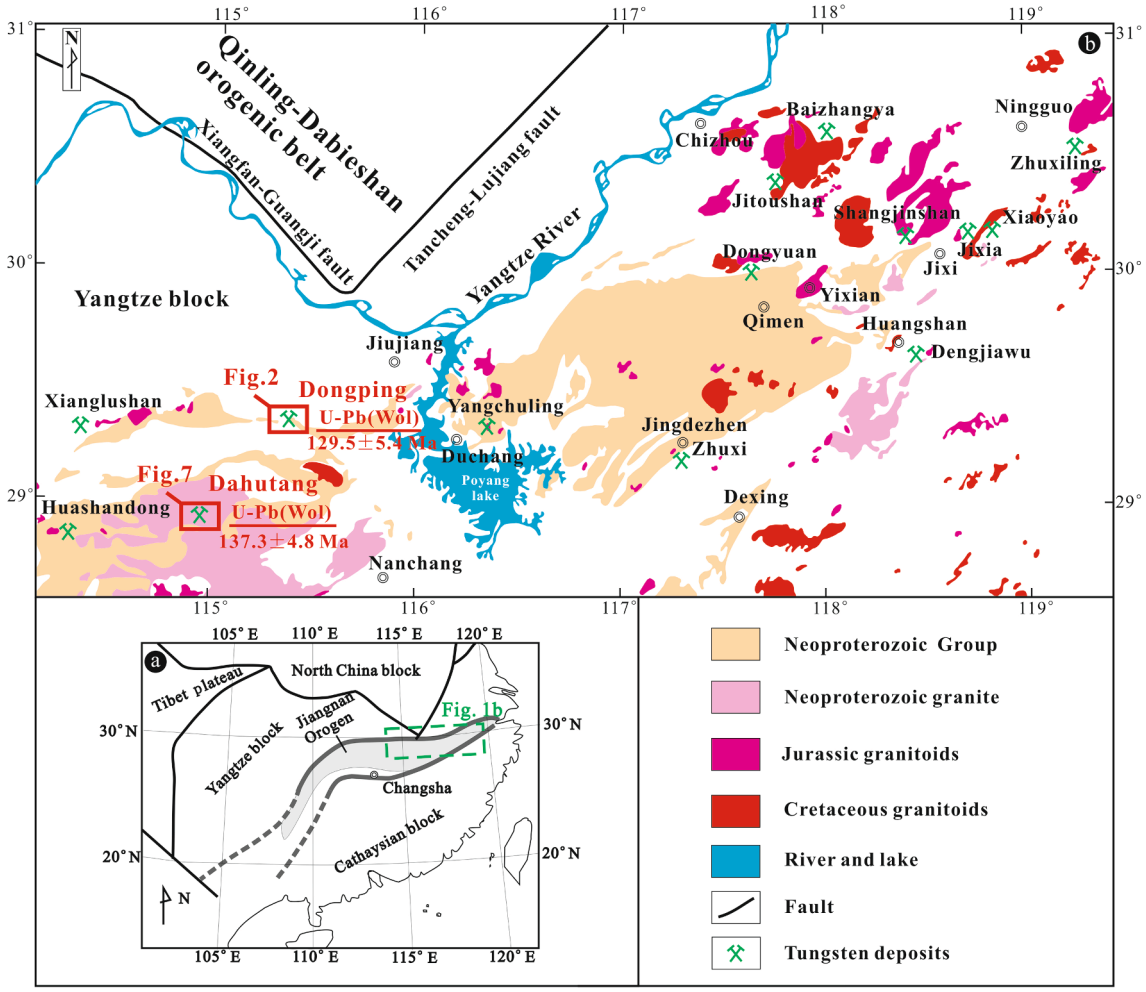

Fig. 1. Sketch map showing the location of the the Jiangnan Orogen, South China (a) and simplified geological map of the Jiangnan tungsten metallogenic belt, showing the distribution of the W deposits (b) (after Mao et al., 2017, 2020; Wu et al., 2019a; Wuet al., 2019b).

timing of mineralization in the quartz-wolframite veins in the JNWB.

Previous studies yielded age constraints on W mineralization in the JNWB, using Re–Os dating of molybdenite (e.g., Feng et al., 2012; Pan et al., 2017), $^{40}Ar/^{39}Ar$ dating of mica (e.g., Pan et al., 2017; Feng et al., 2018), Sm–Nd dating of scheelite (Jiang et al., 2015; Feng et al., 2018), and U–Pb dating of cassiterite (Xu et al., 2015). At present, *in-situ* U–Pb dating of wolframite is feasible and more direct than the dating on gangue minerals (Deng et al., 2019; Harlaux et al., 2018; Tang et al., 2020; Yang et al., 2020a)(, and this method may verify the mineralization ages of the quartz-wolframite-veins in the JNWB.

The Dongping W deposit, which is located about 50 km northwest of Wuning county, northern Jiangxi Province, and is within the western part of the JNWB (Fig. 1b), was discovered by Geological Survey of Jiangxi Province (GSJP) in 2016 (Li et al., 2016). Due to the lack of proper dating of minerals, the age of ore formation and its genetic relationship with the granite are still unclear. The Dahutang W–(Cu–Mo) deposit is situated at the junction of the Wuning, Xiushui and Jingan Counties in northern Jiangxi Province (Fig. 1b). This deposit is dominated by porphyry scheelite ores, followed by large quartz-vein type wolframite ores. These two mineralization styles frequently coexist in space and overlap each other. Most previous studies focused on the ore-forming ages, mineralization mechanisms, and metallogenesis of the scheelite at Dahutang, but few studies on the ore-forming age of wolframite were carried out. In this study, we report the first *in-situ* U–Pb isotope data for wolframite from both the Dongping and Dahutang quartz-vein-wolframite ores in the JNWB, with the aim of: (1) constraining the ore-forming ages of the Dongping and Dahutang wolframite ores and (2) clarifying the relationship between the host granite and wolframite mineralization.

2. Geological background

2.1. Regional geology

The Jiangnan Orogen (Fig. 1a) is a continent–continent collisional belt in South China that was formed initially by the collision of the Yangtze and Cathaysian blocks at 850–820 Ma and subsequently underwent rifting along the Qin–Hang (Qinzhou Bay to Hangzhou Bay) belt. The Jiangnan Orogen extends for ~1500 km along the southeastern margin of the Yangtze Block (Xuet al., 2017), and is made up of

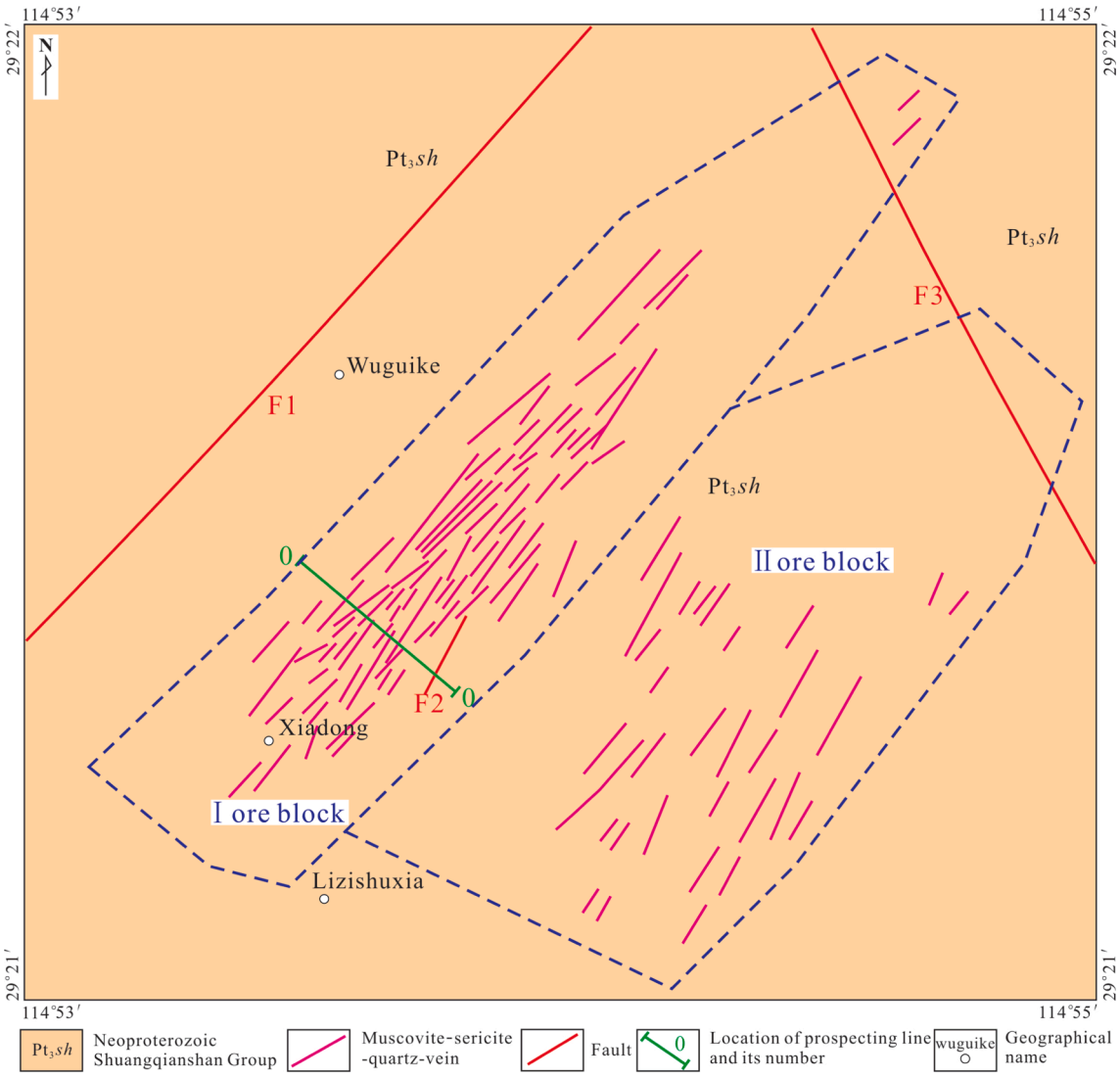

Fig. 2. Geological map of the Dongping ore district (after Hu et al., 2018).

Mesoproterozoic-Early Paleozoic strata and Neoproterozoic and Yanshanian (Late Mesozoic) intrusions and volcanic rocks (Zhang et al., 2017).

Strata in the northeastern margin of the Jiangnan Orogen in northwestern Jiangxi Province include the Neoproterozoic Shuangqiaoshan Group phyllites with few metavolcanic rocks, which are unconformably covered by Silurian to Early Triassic neritic clastic and carbonate rocks, and Middle Triassic to Early Jurassic paralic clastic rocks (Mao et al., 2013). A series of Middle to Late Jurassic-Cretaceous, NE-trending, continental sedimentary basins is developed on these strata.

Two distinct periods of magmatism, represented by the Neoproterozoic and Yanshanian granitic rocks, are recognized in the northeastern margin of the Jiangnan Orogen. The Neoproterozoic Jiuling granitic pluton, the largest composite granitoid complex in southeastern China, has a zircon U–Pb age of ~820 Ma (Zhong et al., 2005) and occupies an outcrop area of >2000 km^2. Zircon U–Pb dating results show that the Late Mesozoic granitic intrusions in this region were emplaced at 151–125 Ma (Feng et al., 2018; Huang and Jiang, 2014; Luo et al., 2010; Mao et al., 2015, 2017; Wang et al., 2015; Zhang et al., 2016; Hu et al., 2018). Previous Re–Os dating of molybdenite, $^{40}Ar/^{39}Ar$ dating of mica, Sm–Nd dating of scheelite, and U–Pb dating of cassiterite suggest that W–Sn mineralization occurred between 150 and 121 Ma (Feng et al., 2012, 2018; Huang and Jiang, 2014; Jiang et al., 2015; Mao et al., 2013; Pan et al., 2017; Xiang et al., 2013a,b; Xu et al., 2015; Zhang et al., 2016).

2.2. Ore deposit geology

2.2.1. The Dongping deposit

The Neoproterozoic Shuangqiaoshan Group is a suite of thick greenschist-facies metamorphic volcanic-clastic sedimentary rocks, including meta-sandstone, meta-siltstone, slate and meta-tuff, which are exposed in the Dongping ore district (Fig. 2). Two NE-trending (F1and F2) and one NW-trending fault (F3) are located in the district, and the NE-trending faults control occurrence of the quartz-wolframite-veins (Fig. 2).

Fig. 3. Photographs of granite samples from the Dongping W deposit. (a-b) medium-grained biotite granite (sample DPBG); (c-d) medium-grained muscovite granite (sample DPMG); (e-f) medium-grained two-mica granite (sample DPTG).

No intrusions outcrop at Dongping, but Early Cretaceous granitic intrusions, which are hidden at 800 to 2000 m below the present surface in the district, include biotite granite, two-mica granite, and muscovite granite (Fig. 3; Li et al., 2016; Yan et al., 2017; Hu et al., 2018). Rock-forming minerals of the biotite granite include plagioclase (ca. 38 vol %), K-feldspar (ca. 25 vol%), quartz (ca. 27 vol%), biotite (ca. 8 vol%) and muscovite (ca. 2 vol%). Except for micas, the contents of rock-forming minerals in the muscovite granite and two-mica granite are similar to those of the biotite granite. The three granite units experienced different degrees of alteration such as K-feldspathization, greisenization and sericitization. These granitic intrusions, which were emplaced at 132–128 Ma, are classified as highly fractionated S-type granites (Li et al., 2016; Li and Li, 2018; Yan et al., 2017; Hu et al., 2018).

The Dongping W deposit contains total metal reserves of as much as 214,000 tons of WO_3 at an average grade of 0.448% and 10,252 tons of Cu at an average grade of 3.64% (GSJP, 2016), making it the largest quartz-vein type wolframite deposit in the world. The Dongping ore bodies, which comprise >300 individual quartz-wolframite ore veins, are mainly hosted in volcanic-clastic sedimentary rocks of the Shuangqiaoshan Group (Li et al., 2016), with minor reserves hosted in hidden Early Cretaceous granitic intrusions. Copper minerals are present in the upper part of the vein systems, whereas wolframite and molybdenite occur at depth (Fig. 4). The Dongping deposit comprises two ore segments, referred to as I and II (Fig. 2); ore segment I is the main one (Hu et al., 2018). Veins in ore segment I strike SE and dip to the south at angles of 50 to 89°. Ore segment I is about 1050 m long, 1018 m deep and 20–250 m wide (Hu et al., 2018). Veins in ore segment II strike NW and dip to the north at angles of 63 to 81°. Ore segment II is about 510 m long, 691 m deep and 40 to 450 m wide. There are five zones between the roof of the granitic pluton and the metamorphic wall rocks (Fig. 4). From bottom to top, these are the pinch-out zone, large vein zone (Fig. 5a, d), thin vein zone (Fig. 5b), veinlet zone (Fig. 5c) and stringer zone (Li et al., 2016), which collectively are known as the five-floor vertical zonation model (Zhang et al., 2017). Overall, the ore veins in the Dongping deposit show an interesting change from the lower to the upper part of this vein system. In the lower part, these veins have widths from 0.05 to 200 cm. In the middle, the widths of the veins range from 2 to 50 cm. Close to the surface, the widths of the veins are the narrowest, ranging from 0.05 to 1 cm wide.

Ore minerals consist of wolframite and chalcopyrite, with small amounts of argentite, bismuthinite, pyrite, pyrrhotite, sphalerite, galena, and arsenopyrite, and minor chalcocite, scheelite and azurite; the gangue minerals consist of quartz and mica (Li et al., 2016; Hu et al., 2018). Wolframite is commonly characterized as coarse- to medium-grained crystals, presents as lath, columnar and irregular shapes (Fig. 5d; Fig. 6a-d), and locally is cut across by galena veins (Fig. 6g). Chalcopyrite often replaces wolframite (Fig. 6i), fills in fractures

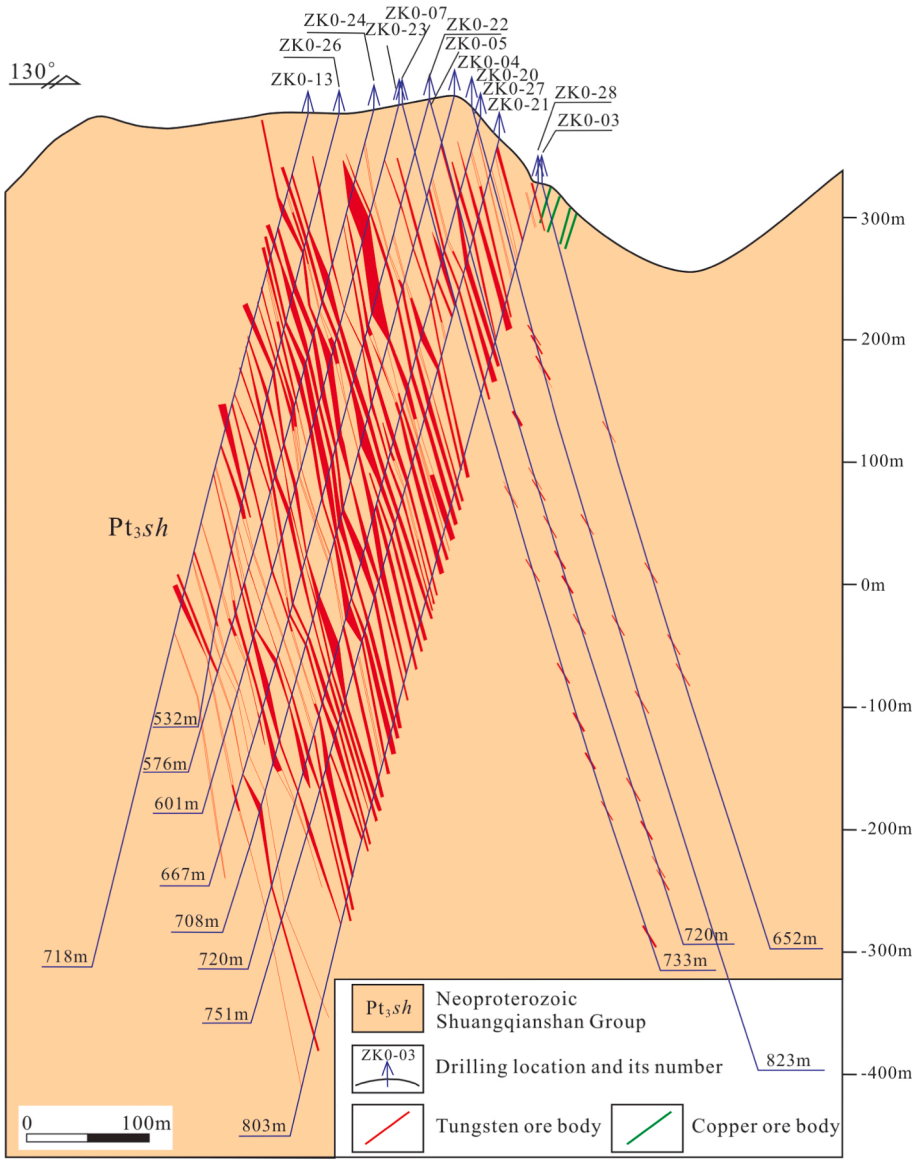

Fig. 4. Geological section along No. 0 exploration line in the Dongping ore district (after GSJP, 2016).

(Fig. 6e), or grows along the margins (Fig. 6f) of wolframite, indicating a later precipitation event. Pyrite occurs around the margins of wolframite as subhedral to euhedral crystals (Fig. 6h).

The emplacement of the hidden Early Cretaceous granitic intrusions at Dongping resulted in thermal metamorphism of the meta-siltstone and slate of the Shuangqiaoshan Group to produce hornfelses in the exo-contact zone (Li et al., 2016). In addition, the hidden granitic intrusions are associated with albitization, greisenization, chloritization, epidotization, sericization, and silicification, as well as with small amounts of mineralization of wolframite, chalcopyrite, molybdenite and pyrite within the endo-contact zone (Li et al., 2016).

2.2.2. *The Dahutang deposit*

The Dahutang W deposit within the western segment of the JNWB hosts an estimated resource of up to 1,100,000 tons of WO_3 at an average grade of 0.185%, 650,000 tons of Cu at an average grade of 0.12% and 80,000 tons of Mo at an average grade of 0.098% (Zhang et al., 2014). This deposit comprises the North Dahutang (Shimensi, Miaowei, Dalingshang), Dawutang (Pingmiao, Dongdouya, Yikuangdai) and South Dahutang (Shiweidong) ore blocks (Fig. 7). At least three mineralization-associated Late Mesozoic granites have been identified on the basis of cross-cutting field relationships combined with zircon age data. These granites include porphyritic granite (porphyritic biotite granite, porphyritic biotite monzogranite, porphyritic muscovite granite and porphyritic two-mica granite), fine-grained biotite (muscovite) granite and biotite granite porphyry, and post-ore granite porphyry, with zircon U–Pb ages ranging from 152 to 137 Ma (Huang and Jiang, 2012; Huang and Jiang, 2013; Huang and Jiang, 2014; Mao et al., 2015; Ye et al., 2016; Zhang et al., 2016; Pan et al., 2017; Feng et al., 2018; Fan et al., 2019; Chu et al.,2019; Chen et al., 2020; Yu et al., 2020).

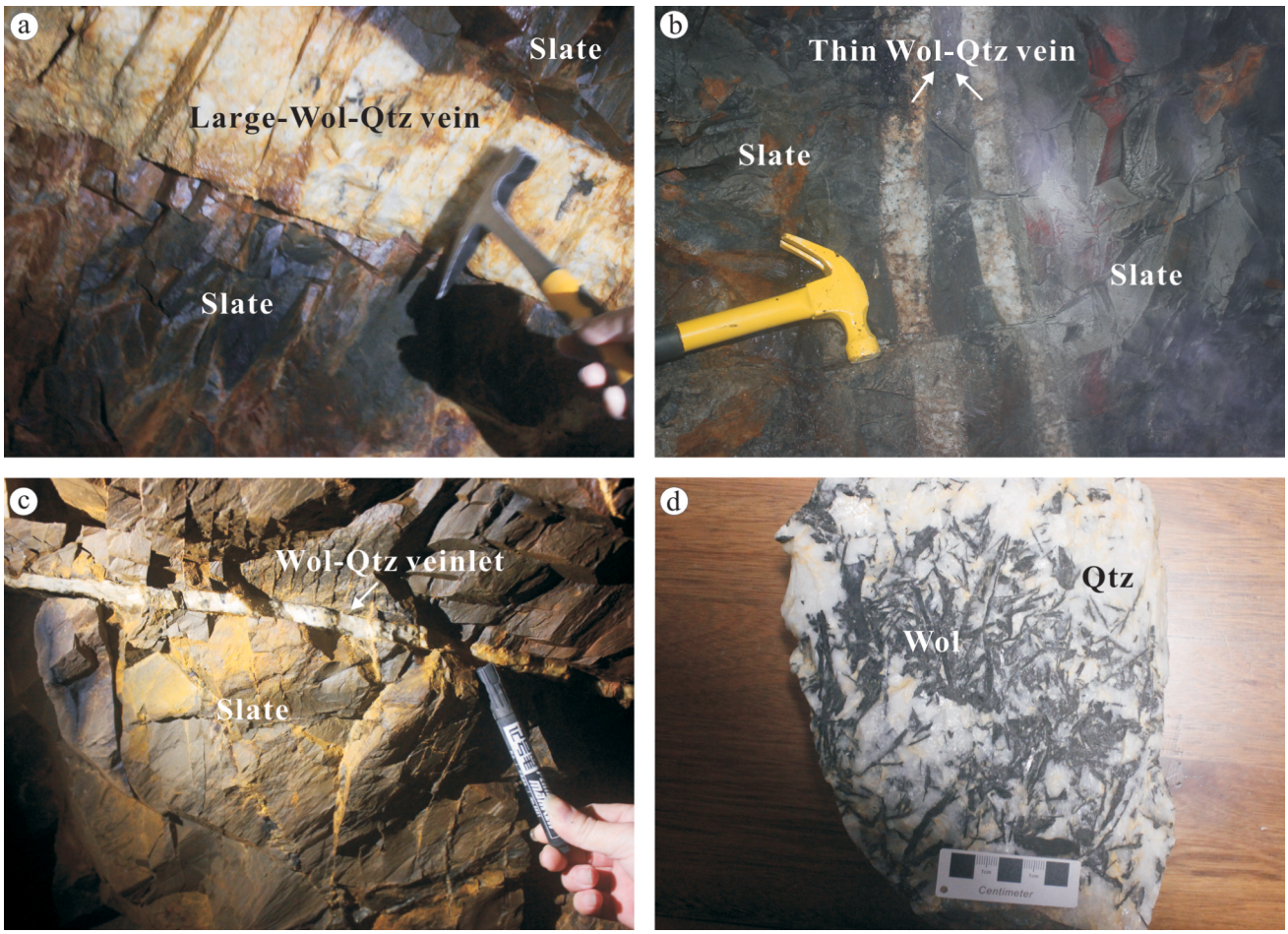

Fig. 5. Photographs of wolframite ores in the Dongping ore district. (a) large quartz-wolframite vein crosscutting the slate (the adit of 295 middle section of the Dongping ore district); (b) thin large quartz-wolframite vein crosscutting the slate (the adit of 295 middle section of the Dongping ore district); (c) quartz-wolframite veinlet crosscutting the slate (the adit of 295 middle section of the Dongping ore district); (d) radial wolframite aggregates in a large quartz vein (mineral collection of the Dongping ore district). Mineral abbreviations: Wol-wolframite; Qtz-quartz.

Three mineralization styles including disseminated-veinlet, large quartz-wolframite-vein and hydrothermal breccia are documented at Dahutang, and these styles frequently coexist in space and overlap each other (Xiang et al., 2013a; Xiang et al., 2013b; Feng et al., 2012; Jiang et al., 2015). Disseminated-veinlet ore bodies occur in the endo-contact or exo-contact zone between the Late Mesozoic granites and Jinningian biotite granodiorites, with a predominance of scheelite in the exo-contact zone. The major ore minerals include scheelite, wolframite and chalcopyrite, with small amounts of molybdenite, pyrrhotite, bornite and pyrite, and the gangue minerals are dominated by quartz, biotite and muscovite (Xiang et al., 2013a). Hydrothermal breccia mineralization occurs at the centre of the mining district and is distributed on top of the porphyritic biotite granite and locally extends to the Jinningian biotite granodiorite batholith (Xianget al., 2013a). Its ore minerals include scheelite, wolframite, chalcopyrite, molybdenite and bornite, with quartz, feldspar, muscovite and fluorite as gangue minerals. Large quartz-wolframite-vein ore bodies are distributed in the central part of the district with an area of about 0.8 km^2 and cut across all the granites and the other ore styles (Xiang et al., 2013a). Ore minerals consist of wolframite, bornite, chalcopyrite, with minor scheelite, chalcocite and pyrrhotite, and the gangue minerals are quartz and muscovite (Fig. 8). The wolframite typically occurs as subhedral, platy or irregular granular crystals that either grew with bornite (Fig. 8b, c, f, h, i) or is locally enclosed by the latter (Fig. 8b, f, g, i). The bornite is often oxidized to form membranes with purple to blue tarnish (Fig. 8a) or is replaced by xenomorphic granular crystals of vein chalcopyrite (Fig. 8b, c, f, h, i). Scheelite occurs as irregular granular crystals and is intimately associated with wolframite and muscovite (Fig. 8d, e). Chalcocite can be observed to be locally present in bornite as emulsion drops (Fig. 8g).

The W mineralization ages of the Dahutang deposit previously obtained from molybdenite Re–Os and muscovite Ar–Ar methods range from 151 to 130 Ma (Feng et al., 2012; Mao et al., 2013; Xiang et al., 2013b; Zhang et al., 2016; Song et al., 2018). The ore-forming fluids have high to medium temperatures (310–370 °C, peak at 330–350 °C) and low salinities (1.6 to 9.6 wt% NaCl equiv.), and contain CH_4, N_2 and/or CO_2. This indicates that the fluids were derived from granitic magma with minor input of meteoric water and that fluid-rock interaction was critical for scheelite deposition (Peng et al., 2018).

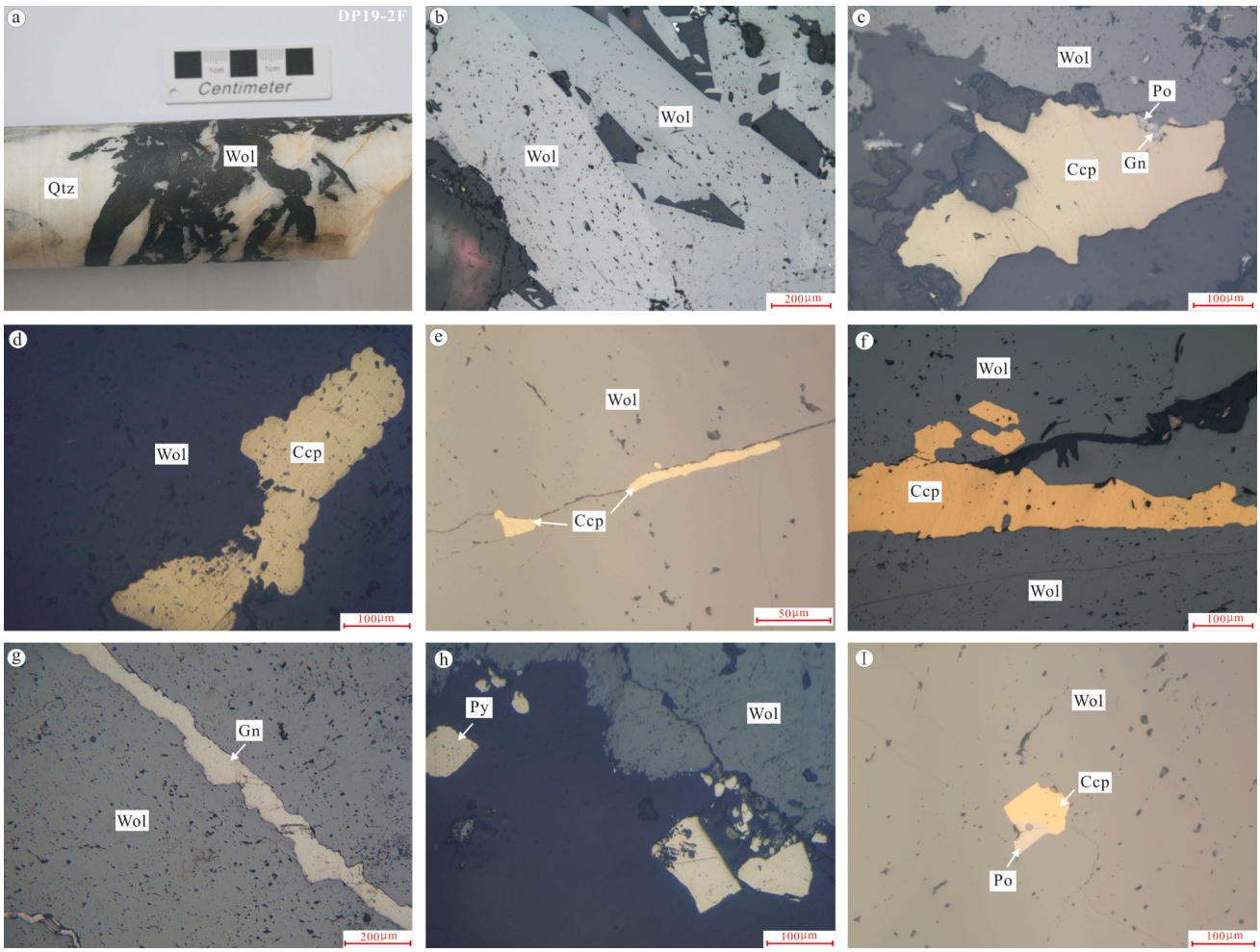

Fig. 6. The hand specimen photograph (a) and photomicrographs (b-i, reflected light) of the ores from the Dongping W deposit. (a) The ~2 cm wolframite crystal wolframite in tabular; (b) the coarse crystals wolframite in tabular and coexists with quartz; (c) wolframite coexists with chalcopyrite, and minor pyrrhotite and gelenite; (d) wolframite coexists with chalcopyrite; (e) chalcopyrite fills along the fractures in wolframite; (f) chalcopyrite fills at the margins of wolframite; (g) gelenite veins interspersed with wolframite; (h) pyrite fills at the margins of wolframite; (i) chalcopyrite coexists with pyrrhotite, and replaced wolframite. Mineral abbreviations: Ccp-chalcopyrite; Gn-gelenite; Po-pyrrhotite; Py-pyrite; Wol-wolframite; Qtz-quartz.

3. Sampling and analytical methods

3.1. Sampling

Three granite samples (DPBG, DPMG, DPTG) were collected underground at the Dongping W deposit for zircon U–Pb dating (Fig. 3). Samples DPBG (medium-grained biotite granite) and DPMG (medium-grained muscovite granite) were collected from the hidden pluton at depths of 1093 m and 910 m, respectively, in drill hole ZK6-50, and sample DPTG (medium-grained two-mica granite) was collected from the hidden pluton at a depth of 923 m in drill hole ZK5050. After crushing the rock samples, zircon grains were separated using standard heavy liquid and magnetic separation techniques.

Wolframite samples DP19-2F and DHT-1T were extracted from representative quartz-wolframite-veins in the Dongping and Dahutang deposits, respectively. Sample DP19-2F is from a quartz-wolframite vein with a width of ~5 cm at the 500 m level in drill hole ZK5050 (Fig. 6a). The mineral assemblage of sample DP19-2F consists of wolframite, quartz, pyrite and chalcopyrite (Fig. 6b-i), and the wolframite is coarse-grained with a length of 2–5 cm and a width of 0.5–1 cm. Sample DHT-1 T was collected from a large quartz-wolframite-vein about 10 cm wide that was observed at 565.08 m in drill hole ZK10409 in the Miaowei ore block of the Dahutang deposit (Fig. 8a). The mineral assemblage of this sample consists of wolframite with relatively large grain sizes (~10 cm in length by ~5 cm in width), quartz, pyrite and bornite (Fig. 8b-i). Therefore, it was possible to directly handpick wolframite separates under a binocular microscope, after which they were mounted in 25 mm-diameter epoxy mounts and polished.

3.2. Zircon LA-ICP-MS in-situ U–Pb dating

Zircon grains were extracted by conventional heavy-liquid and magnetic-separation techniques and then manually selected under a binocular microscope at the mineral-separation laboratory of

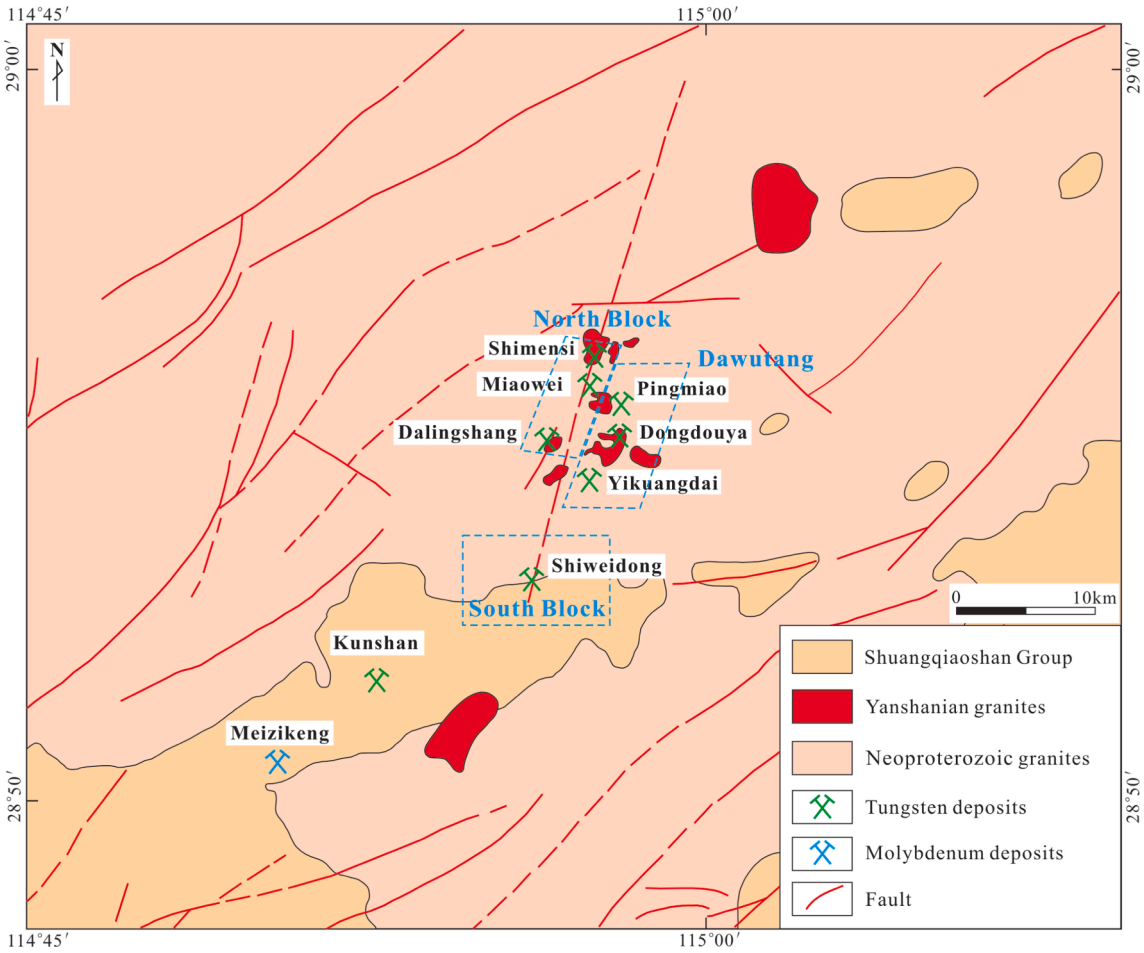

Fig. 7. Simplified geological map of the Dahutang W deposit that includes North Dahutang, Dawutang and South Dahutang ore blocks (after Wei et al., 2017; Jiang et al., 2015).

Hongchuang Geological Exploration Technology Service Co., Ltd. (NHEXTS), Nanjing, China. Cathodoluminescence (CL) imaging was performed using a Tescan MIRA 3LMH Schottky field-emission scanning electron microscope (SEM) at the NHEXTS. U–Pb dating and trace element analyses of zircon were conducted simultaneously by laser ablation ICP-MS (LA-ICP-MS) at the NHEXTS. A RESOlution S-155 193 nm excimer laser-ablation system (Australian Scientific Instruments, Canberra, Australia) and Agilent 7700x quadrupole ICP-MS (Hachioji, Tokyo, Japan) were used together for the experiments. The laser beam, homogenized by a set of beam delivery systems, was focused on the zircon surface with flux of 3.5 J/cm^2. The ablation protocol employed a spot diameter of 33 μm at 5 Hz repetition rate for 40 s (equating to 200 pulses). Helium was used as the carrier gas to efficiently transport aerosol to the ICP-MS. Zircon 91500 was the external standard used to correct instrumental mass discrimination and elemental fractionation during the ablation. Zircon GJ-1 was used as the quality control for geochronology. Fifteen analyses of GJ-1 yielded $^{206}Pb/^{238}U$ concordant ages of 602.6 ± 2.6 Ma, which is equal within uncertainty to its recommended value of 599.4 ± 2.5 Ma (Jackson et al., 2004). Analyses of all trace elements of zircon were calibrated against NIST SRM 610 with Zr as internal standard for other trace elements (Hu et al., 2011). The average analytical error ranges from ±10% for light REEs (LREE) to ±5% the other REEs. Detailed operating conditions for the laser ablation system and the ICP-MS instrument and data reduction are the same as outlined by (Liu et al., 2010a,b). ICPMSDataCal software 10.0 (Liu et al., 2010a,b) was used for off-line selection and integration of background and analytical signals and for time-drift correction and quantitative calibration for trace element analyses and U–Pb dating. Concordia diagrams and weighted mean age calculation were made using Isoplot 3.0 (Ludwig, 2003). The errors of individual LA-ICP-MS analyses are reported at the 90% (2σ) confidence level.

3.3. *In-situ chemical compositions of wolframite by EPMA*

Electron microprobe analyses (EPMA) of major elements in wolframite were performed at the State Key Laboratory of Geological Processes and Mineral Resources, China University of Geosciences (Wuhan), with a JEOL JXA-8230 Electron Probe Micro Analyzer equipped with five wavelength-dispersive spectrometers (WDS). The samples were coated with a thin conductive carbon film prior to analysis. During the analysis, an accelerating voltage of 15 kV, a beam current of 20 nA and a 1 μm spot size were used to analyze minerals.

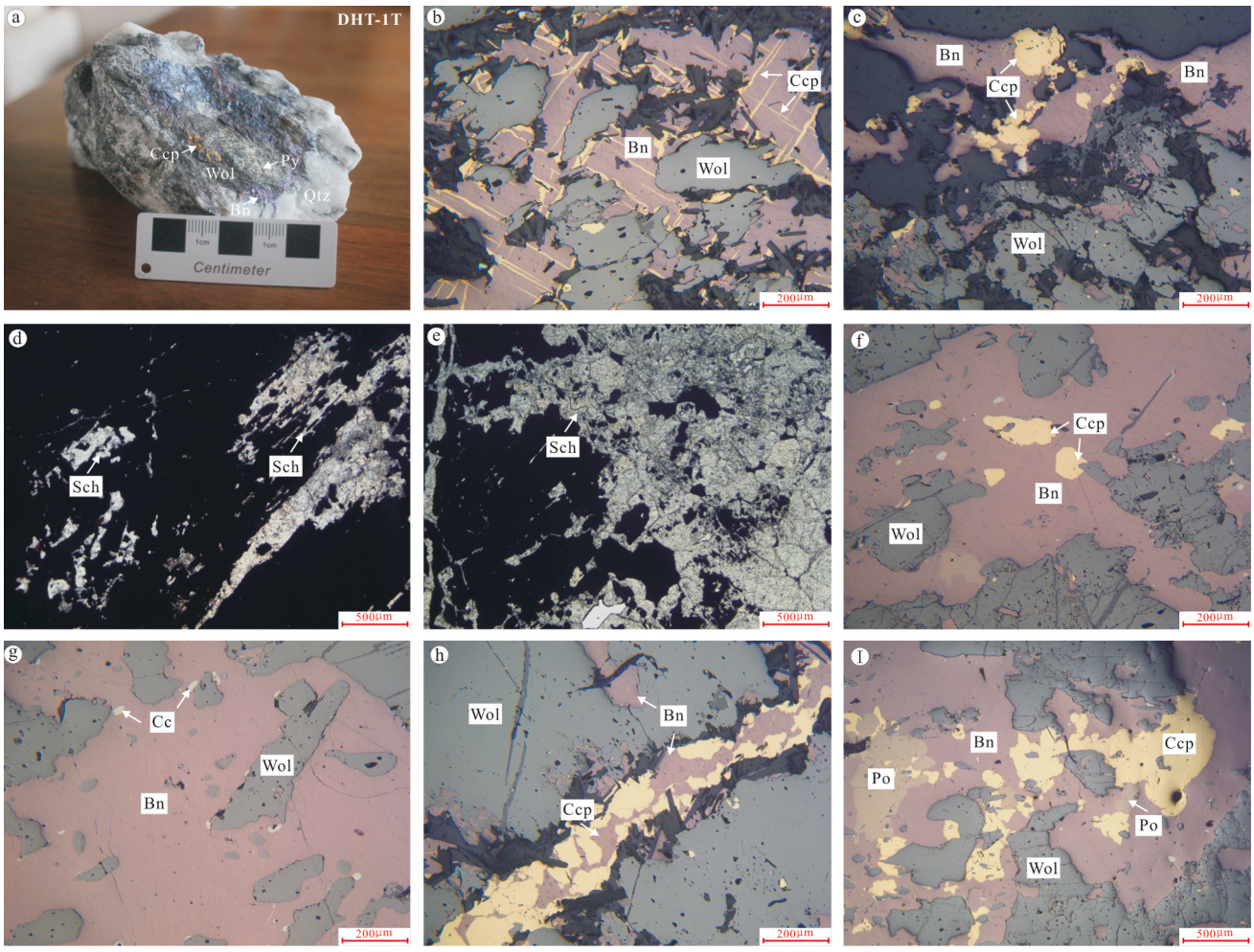

Fig. 8. The hand specimen photograph (a) and photomicrographs (b-i, reflected light) of the ores from the Dahutang W deposit. (a) hand specimen of the quartz-vein wolframite, bornite was oxidized and form the purple blue tarnish membrane; (b) wolframite is enclosed by bornite and bornite was replaced by latticed chalcopyrite; (c) wolframite coexists with bornite and bornite was replaced by chalcopyrite; (d-e) scheelite coexists with wolframite; (f) wolframite coexists with bornite and/or is locally enclosed by bornite, with bornite was replaced by irregular granular chalcopyrite; (g) wolframite is enclosed by bornite, and chalcocite locally distributed in bornite in the form of emulsion drops; (h) wolframite coexists with bornite, with bornite was replaced by vein chalcopyrite; (i) wolframite coexists with bornite and/or is locally enclosed by bornite, with bornite was replaced by irregular granular chalcopyrite and pyrrhotite; Mineral abbreviations: Bn-bornite; Cc-chalcocite; Ccp-chalcopyrite; Po-pyrrhotite; Py-pyrite; Sch-scheelite; Wol-wolframite; Qtz-quartz.

Data were corrected on-line using a ZAF (atomic number, absorption, fluorescence) correction procedure. The peak counting time was 10 s for W, Mn, Fe, and Nb. The background counting time was one-half of the peak counting time on the high- and low-energy background positions. The following standards were used: tungsten (W), manganese (Mn), hematite (Fe), and niobium (Nb).

3.4. *In-situ LA-SF-ICP-MS U–Pb dating on wolframite*

In order to identify the internal textures of wolframite crystals and thus to improve the interpretation of U-Pb ages, backscattered electron (BSE) images of wolframite from samples DP19-2F and DHT-1T were photographed by using a JSM-7800F field emission scanning electron microscope at the State Key Laboratory of Geological Processes and Mineral Resources, China University of Geosciences, Wuhan, China.

U–Pb dating of wolframite was carried out by LA-SF-ICP-MS at the State Key Laboratory of Ore Deposit Geochemistry (SKLODG), Institute of Geochemistry, Chinese Academy of Sciences (IGCAS), Guiyang, China, using an Agilent 7900 ICP-MS and a Thermo Scientific Element XR sector field ICP-MS equipped with a GeoLasPro 193 nm ArF excimer laser. Analytical conditions and methods have been reported in (Tang et al., 2020, 2021). The data collected from ICP-MS were processed off-line using the ICPMSDataCal software for calibration, background correction, and drift correction of the integrated signal. Isoplot 4.15 was used to calculate the U–Pb ages and draw concordia diagrams. Analytical errors for isotopic ratios in the samples are reported at the 1σ level.

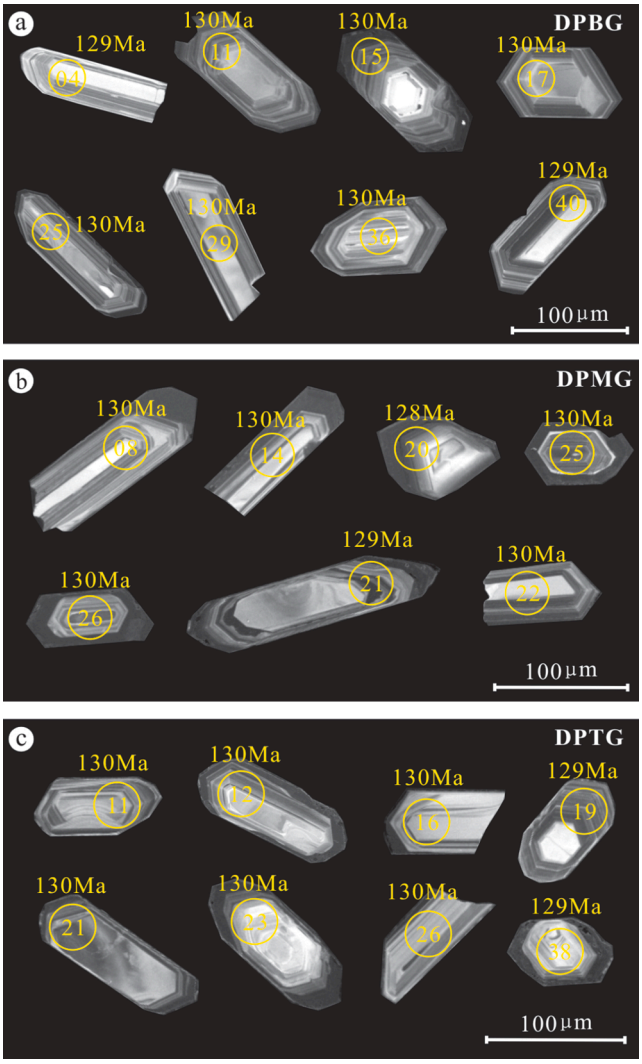

Fig. 9. Representative cathodoluminescence images for zircon grains of granite samples from the Dongping W deposit.

4. Results

4.1. Zircon U–Pb ages

Zircon grains in the medium–grained biotite granite sample DPBG are euhedral with widths of 30–100 μm and lengths of 50–300 μm (Fig. 9a). Most of these zircon grains have clear and bright oscillatory zonation in cathodoluminescence (CL) images, indicating a magmatic origin (Wilde et al, 2001). The muscovite granite sample DPMG has zircon grains with lengths of 30–150 μm and widths of 30–80 μm (Fig. 9b). Zircon grains that appear turbid and black in CL images are more abundant than bright and clear ones. The zircon grains from the two-mica granite sample DPTG have lengths of 30–200 μm and widths of 30–80 μm (Fig. 9c). Again, turbid and black zircon grains in CL images are more abundant than bright and clear ones. Based on detailed statistics of zircon grains in CL and BSE images, the grains become smaller and the proportion of grains with a bright and clear appearance in CL images decreases going from the biotite granite, to the two-mica granite, and to the muscovite granite. U–Pb isotope analyses were conducted only on zircon grains with bright CL images, clear zonation, and without mineral inclusions and cracks. The LA-ICP-MS analytical data are summarized in Appendix 1. The error on individual analyses is reported at the 2σ level, and the weighted mean $^{206}Pb/^{238}U$ ages are quoted at the 95% confidence level.

Twenty-one spots on different magmatic zircon grains of sample DPBG (biotite granite) were measured. These zircon grains have U and Th contents 211–3268 ppm and 45–865 ppm, respectively, and the Th/U ratios range from 0.02 to 0.92. They yield a weighted mean $^{206}Pb/^{238}U$ age of 129.8 ± 0.5 Ma (2σ, MSWD = 0.62) (Fig. 10a, b). This age represents the emplacement age of the biotite granite.

Twenty magmatic zircon grains were analyzed from sample DPMG (muscovite granite). These zircon grains have Th and U contents 26–776 ppm and 413–1503 ppm, respectively, and the Th/U ratios range from 0.03 to 1.57. They yield a weighted mean $^{206}Pb/^{238}U$ age of 129.8 ± 0.5 Ma (2σ, MSWD = 0.35) (Fig. 10c, d), which represents the crystallization age of the muscovite granite.

Twenty-seven spots on different magmatic zircon grains were analyzed from sample DPTG (two-mica granite). These zircon grains have variable Th and U contents ranging from 52 to 3925 ppm and 241–3110 ppm, respectively, and the Th/U ratios range from 0.04 to 1.42. The weighted mean $^{206}Pb/^{238}U$ age is 129.7 ± 0.4 Ma (2σ, MSWD = 0.3) (Fig. 10e, f), which is interpreted as the emplacement time of the two-mica granite.

4.2. Textures and major element compositions of wolframite

Wolframite samples DP19-2F and DHT-1T from the Dongping and Dahutang deposits, respectively, show homogeneous internal textures, and no obvious zoning or growth generations were observed under backscattered electron imaging (BSE) (Fig. 11).

The major element compositions of the wolframite separates from the Dongping and Dahutang deposits determined by EPMA are given in Appendix 2. Wolframite from sample DP19-1F has higher FeO contents (14.09–21.36 wt%) than sample DHT-2T (9.96–15.54 wt%), whereas sample DP19-1F has a lower MnO content (3.17–10.44 wt%) than sample DHT-2 T (7.54–12.82 wt%). Wolframite samples DP19-1F and DHT-2T are Fe-rich with Fe/(Fe + Mn) values of 0.43–0.87, which is close to the ferberite end member (Fig. 12).

4.3. Wolframite U–Pb ages

Wolframite *in-situ* U–Pb isotope data for selected samples from the Dongping and Dahutang deposits are presented in Appendix 3 and described below.

Thirty spot analyses on wolframite sample DP19-2F from the Dongping W deposit have total Pb, Th and U concentrations ranging from 0.1 to 0.6, 0.1 to 30.0 and 0.1 to 16.4 ppm, respectively. A lower intercept $^{206}Pb/^{238}U$ age of 129.5 ± 5.4 Ma (1σ, MSWD = 0.75) was obtained from the Tera-Wasserburg concordia diagram (Fig. 13a).

Thirty-four spot analyses were performed on wolframite sample DHT-1T with total Pb of 0.1–1.6 ppm, Th of 0.0–0.2 ppm and U of 0.7–5.1 ppm (averaging 1.8 ppm). These spots yielded a lower intercept $^{206}Pb/^{238}U$ age of 137.3 ± 4.8 Ma (1σ, MSWD = 1.7) in the Tera-Wasserburg concordia diagram (Fig. 13b).

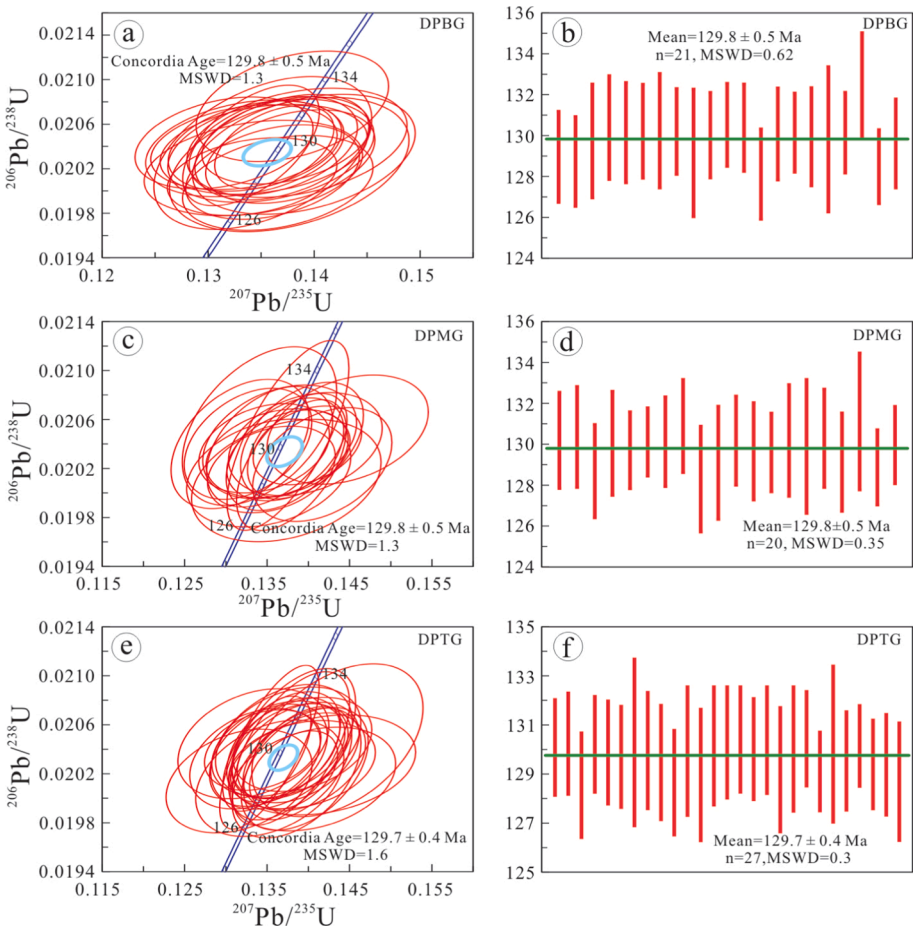

Fig. 10. Zircon U–Pb concordia plots and weighted mean age diagrams for granites in the Dongping W deposit.

5. Discussion

5.1. Age of emplacement of the hidden granite pluton in Dongping

Yan et al (2017) reported a zircon LA-ICP-MS U–Pb age of 128.7 ± 0.8 Ma for the muscovite granite of the hidden pluton in the Dongping deposit. In addition, LA-ICP-MS dating of zircon in the biotite granite of the hidden pluton gave a U–Pb age of 132.9 ± 1.4 Ma (Hu et al., 2018).

Our new LA-ICP-MS U–Pb data define a precise $^{206}Pb/^{238}U$ age of 129.8 ± 0.3 Ma (2σ, MSWD = 0.4), which is weighted average from samples of the three granite units. The individual ages of these granite units (biotite granite, muscovite granite and two-mica granite of the hidden pluton in the Dongping deposit) overlap within the analytical error. The new age is consistent with the published LA-ICP-MS U–Pb data within their analytical errors (Yan et al., 2017; Hu et al., 2018). Therefore, our new LA-ICP-MS zircon U–Pb dating of biotite granite, muscovite granite and two-mica granite defines an emplacement age of 129.8 ± 0.3 Ma for the hidden pluton in the Dongping deposit.

5.2. Mineralization ages of the Dongping and Dahutang deposits

5.2.1. The Dongping deposit

In this study, a lower intercept $^{206}Pb/^{238}U$ age of 129.5 ± 5.4 Ma (Fig. 13a) was obtained from *in-situ* U–Pb dating of wolframite from the Dongping deposit. It is noteworthy that the obtained lower intercept $^{206}Pb/^{238}U$ age is coeval within the analytical error with that of the hidden Dongping granitic intrusions obtained in this study. Thus, the obtained lower intercept $^{206}Pb/^{238}U$ age of 129.5 ± 5.4 Ma is reliable and can be considered to represent the formation age of wolframite ore in the Dongping deposit. Therefore, we propose that the Dongping deposit is both spatially and temporally related to the hidden granitic intrusions. This interpretation corresponds with the geological evidence, for example, the occurrence of minor wolframite, chalcopyrite and molybdenite mineralization in veins within the endo-contact zone (Li et al., 2016).

5.2.2. The Dahutang deposit

The previously reported W mineralization ages for the Dahutang deposit, most of which were obtained from Re-Os dating of the ore

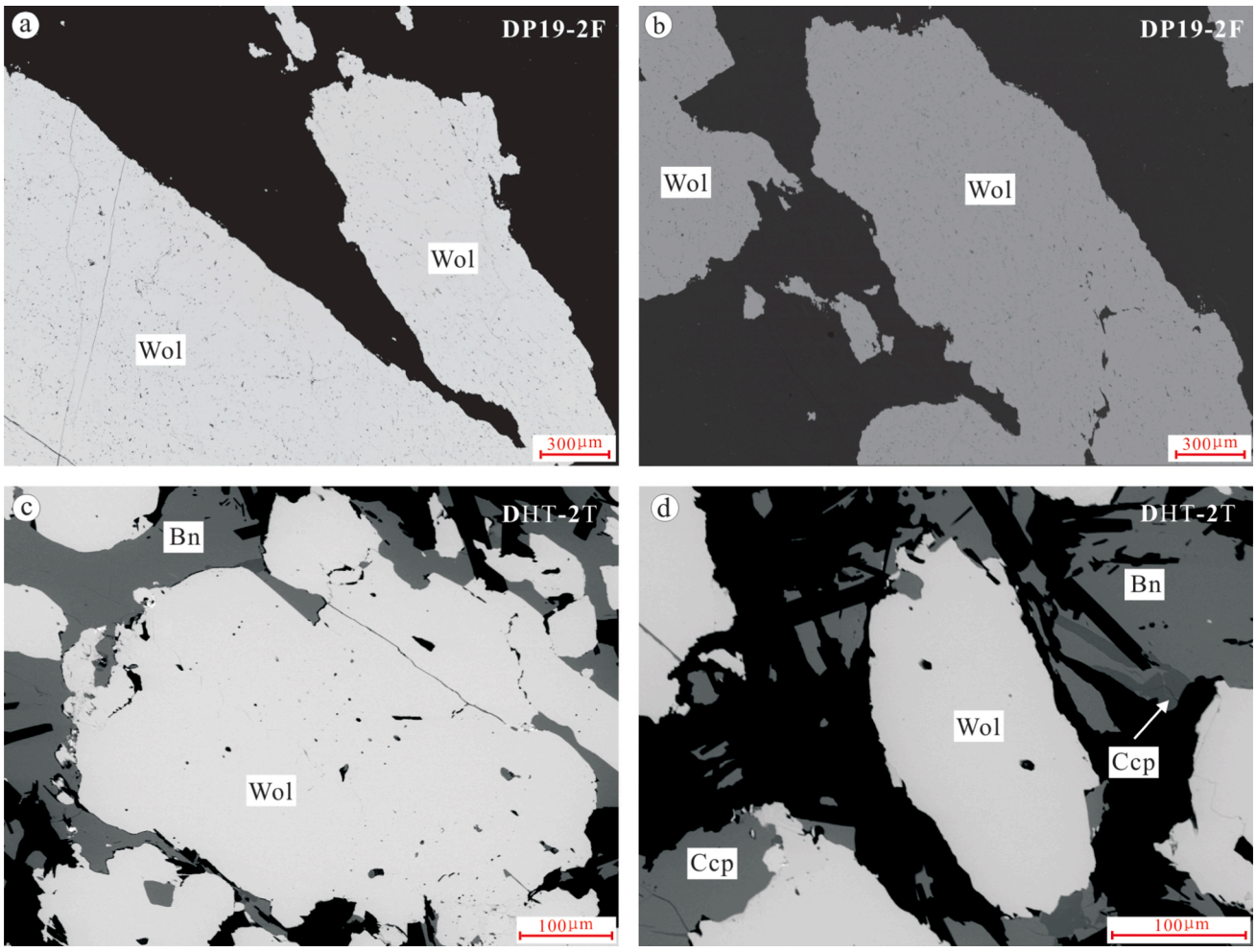

Fig. 11. U–Pb dating of wolframite sample DP19-2F from the Dongping W deposit, wolframite is mainly intergrowth with quartz and occurs as coarse crystals in tabular (a-b) (BSE image) and sample DHT-2T from the Dahutang W deposit, wolframite is mainly intergrowth with quartz and occurs in veins as coarse crystals in tabular (c-d) (BSE image).

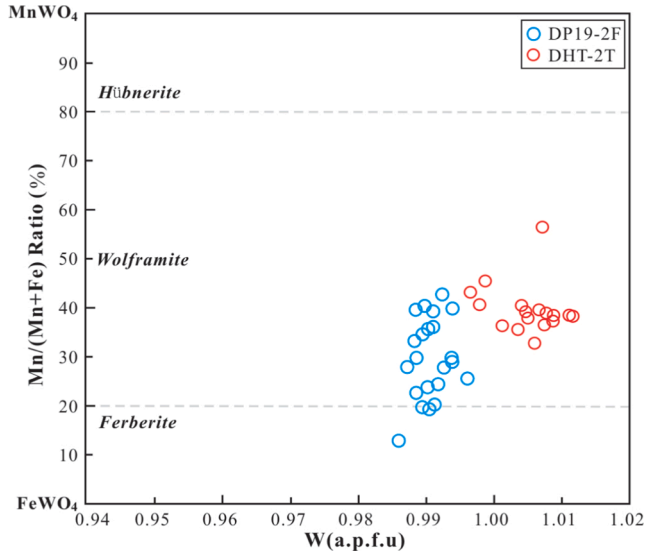

Fig. 12. Major element composition of the wolframite samples from the Dongping and Dahutang W deposits. The variation in Mn/(Fe + Mn) shows the compositional range between the manganese-rich endmember hubnerite and the iron-rich endmember ferberite.

minerals molybdenite and scheelite, range from 151.0 ± 1.3 Ma to 137.9 ± 2.0 Ma (Fig. 14a) (Feng et al., 2012, 2018; Jiang et al., 2015; Mao et al., 2013; Xiang et al., 2013b; Zhang et al., 2013, 2016, 2017; Lin et al., 2021). Xiang et al (2013) obtained a molybdenite Re–Os age of 149.6 ± 1.4 Ma for the quartz + molybdenite + chalcopyrite + wolframite + minor scheelite vein ores in the Shimensi ore block. Zhang et al. (2016) and Lin et al. (2021) reported molybdenite Re–Os ages of 151.0 ± 1.3 Ma and 148.8 ± 1.0 Ma, respectively, for the quartz + wolframite + chalcopyrite + molybdenite vein ores in the Kunshan ore block. A similar molybdenite Re–Os age of 148.9 ± 4.4 Ma was also found for the quartz + molybdenite + chalcopyrite vein ores in the Meizikeng ore block (Zhang et al., 2013). These ages are consistent with previously published zircon/monazite U–Pb ages for the porphyritic biotite granite and porphyritic biotite monzogranite in the Dahutang mining district, i.e., 148.3 ± 2.6 Ma, 147.9 ± 1.1 Ma, 148.3 ± 1.9 Ma, 148.8 ± 2.4 Ma, 150.7 ± 0.7 Ma and 151.7 ± 1.3 Ma (Fig. 8a) (Chu et al., 2019; Fan et al., 2019; Mao et al., 2015; Pan et al., 2017; Ye et al., 2016; Zhang et al., 2016). Therefore, the Dahutang deposit yields a ca. 150 Ma age for the W-Cu-Mo mineralization, which is characterized by quartz + wolframite + chalcopyrite + molybdenite vein ores and is most likely related to the emplacement of porphyritic biotite granite and biotite monzogranite.

However, a younger ore-forming age group of ca. 140 Ma has also been recognized for the Dahutang W-Cu-Mo mineralization (Fig. 14a). Feng et al (2012) obtained a molybdenite Re–Os age of 140.9 ± 3.6 Ma for the quartz + chalcopyrite + molybdenite + wolframite ± scheelite

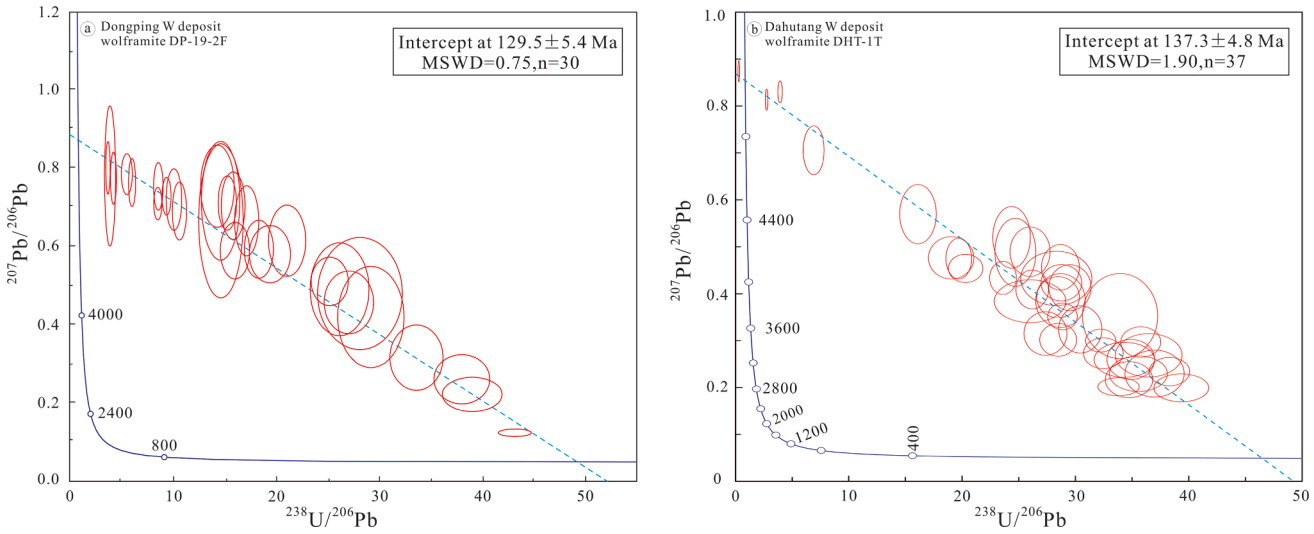

Fig. 13. Tera-Wasserburg plots and the lower intercepts ages of wolframite samples from the Dongping (a) and Dahutang (b) W deposit (Using NIST612 or 614 and MTM for calibration of Pb-Pb and U-Pb ratios, respectively).

vein ores in the Shiweidong ore block. Mao et al (2013) reported a molybdenite Re–Os age of 139.2 ± 1.0 Ma for the disseminated-veinlet, hydrothermal breccia and large quartz-vein type scheelite + chalcopyrite + molybdenite + wolframite ores in the Shimensi ore block. Similarly, the quartz + scheelite + molybdenite + chalcopyrite vein ores in the Dawutang ore block produced a molybdenite Re–Os age of 137.9 ± 2.0 Ma (Zhang et al., 2017). In addition, Jiang et al. (2015) obtained scheelite Sm–Nd isochron ages of 142.4 ± 8.9 Ma for the quartz + scheelite + wolframite + chalcopyrite ores in the Shiweidong ore block. Our new wolframite *in-situ* U–Pb age of 137.3 ± 4.8 Ma (Fig. 13b) is consistent with the previous scheelite Sm–Nd and molybdenite Re–Os ages for the Dahutang mineralization as well as the zircon/monazite U–Pb ages of 138.6 ± 1.0 Ma, 142.8 ± 1.7 Ma and 143.7 ± 2.4 Ma for the emplacement of the fine-grained biotite granite and granite porphyry (Fig. 14a; Fan et al., 2019; Chu et al., 2019). Therefore, it is clear that there is a younger W–Cu mineralization age at ca. 140 Ma in the Dahutang deposit, which is associated with porphyry-type scheelite ores and quartz-vein type wolframite and chalcopyrite ores, and is related to the fine-grained biotite granite and granite porphyry. Consequently, we suggest that the Dahutang deposit is the product of two W–Cu–Mo mineralization stages.

5.3. *Two significant quartz-wolframite-vein mineralization events in the JNWB*

Previous studies have recognized two important periods of porphyry and skarn scheelite mineralization in the JNWB the Late Jurassic–Early Cretaceous (150–135 Ma) and Cretaceous (130–125 Ma) (Mao et al., 2020). The early period of porphyry, skarn and porphyry-skarn W–Cu–Mo mineralization was predominant in the JNWB, and resulted in a series of ore deposits including Dahutang, Yangchuling, Zhuxi, Dongyuan and Baizhangyan, with ore-forming ages clustering between ca. 147 and 140 Ma (Fig. 14b). The late period (130–125 Ma) of Sn–W mineralization generated skarn- and quartz-vein type ores represented by the Xianglushan W and Jianfengpo Sn deposits, and has ore-forming ages clustering at ca. 126 Ma.

In the present study, we also confirm two significant wolframite mineralization events at ca. 140 Ma and ca. 130 Ma in light of precise *in-situ* U–Pb dating of wolframite from the Dongping and Dahutang deposits in the JNWB. The early stage (ca. 140 Ma) of quartz-wolframite veining occurs as a subordinate ore style in the porphyry and skarn scheelite deposits including Dahutang, Shangjinshan and Dawujian. As for the late stage (ca. 130 Ma) of quartz-wolframite vein mineralization, the Dongping deposit is the only representative that has so far been discovered in the JNWB. Notably, the late stage of quartz-wolframite vein-type mineralization is promising for future exploration strategies in the JNWB.

6. Conclusions

(1) The main ore minerals in the Dongping deposit are wolframite and chalcopyrite, with small amounts of argentite, bismuthinite, pyrite, pyrrhotite, blende, galena and arsenopyrite. LA-ICP-MS zircon U–Pb dating of biotite granite, muscovite granite and two-mica granite defined an emplacement age of 129.8 ± 0.3 Ma for the hidden pluton in the Dongping deposit. *In-situ* U–Pb dating of wolframite yielded a lower intercept $^{206}Pb/^{238}U$ age of 129.5 ± 4.8 Ma, which is coeval within analytical error with the genetically related granitic intrusions.

(2) *In-situ* U-Pb dating of wolframite from the Dahutang deposit by LA-SF-ICP-MS yielded a lower intercept $^{206}Pb/^{238}U$ age of 137.3 ± 4.8 Ma. We thus confirm that there is a ca. 140 Ma quartz-wolframite-chalcopyrite-vein mineralization event in the Dahutang deposit.

(3) The ore-forming ages of ca. 140 Ma and ca. 130 Ma obtained by direct dating of wolframite from the Dahutang and Dongping deposits confirm that two significant quartz-wolframite-vein mineralization events occurred in the JNWB.

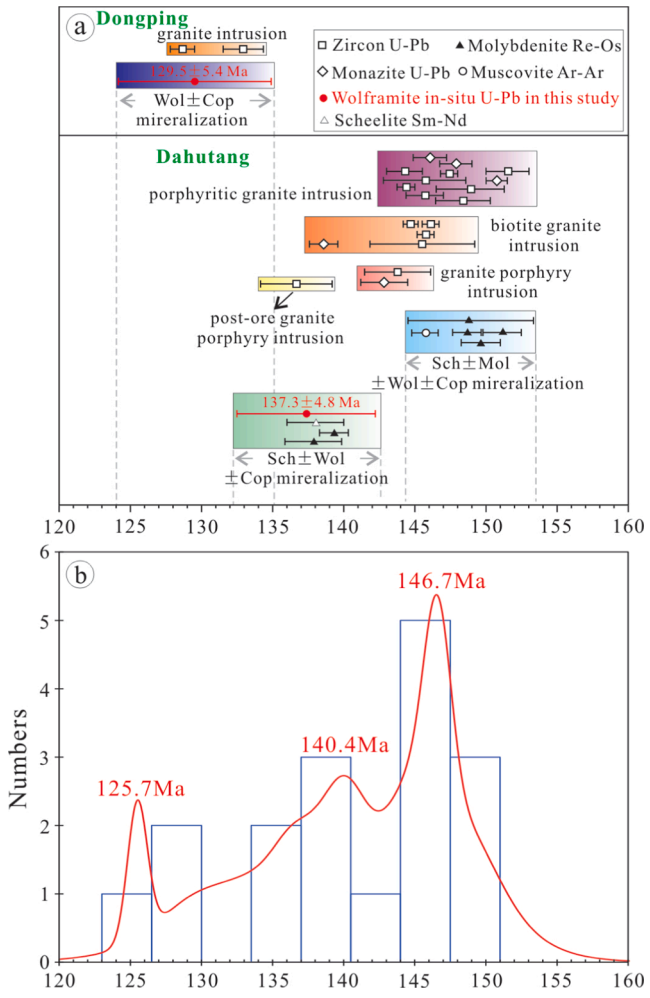

Fig. 14. Comparison of wolframite U–Pb ages obtained in this study with previously published ages of granitic intrusions and the ore-forming for the Dongping and Dahutang W deposit (a) (Chu et al., 2019; Fan et al., 2019; Feng et al., 2012, 2018, Huang and Jiang, 2012, 2014; Mao et al., 2013; Pan et al., 2017; Xiang et al., 2013a,b; Yan et al., 2017; Ye et al., 2016; Yu et al., 2020; Zhang et al., 2013, 2016, 2017; Hu et al., 2018; Lin et al., 2021) from the Dongping and Dahutang deposits, and probability density plots generated by the previously published ages of hydrothermal W mineralization (b) in the JNWB (data from ages reviewed by Mao et al., 2020; Song et al., 2012a,b; Tang et al., 2019; Zhang et al., 2013). The episodes for age probability density were identified by the mixing age separating model (Vermeesch, 2012). Mineral abbreviations in Fig. 14a: Sch-scheelite; Wol-wolframite;.Mol-molybdenite; Cop-copper.

Declaration of Competing Interest

The authors declare that they have no known competing financial interests or personal relationships that could have appeared to influence the work reported in this paper.

Acknowledgments

We thank associate research fellow Shenghua Wu of the Chinese Academy of Geological Sciences, professor Jiajing Zhang of Jiangxi College of Applied Technology, Professor of Engineering Xianguang Wang of Jiangxi Mineral Resources Guarantee Service Center, Professor of Engineering Fangrong Zhang and Jiming Li of Geological Survey of Jiangxi Province for their help for the article. We also thank associate research fellow Fabin Pan of China University of Geosciences (Wuhan) for his help with electron microprobe analyses. This research was jointly supported by grants from the National Natural Science Foundation of China (No. 41930428 and No. 41802042), Science and Technology Award Reserve Project Cultivation Program of Science and Technology Department of Jiangxi Province (No. 20203AEI91004), the open fund of State Key Laboratory of Nuclear Resources and Environment (No. 2020NRE16) and the Doctoral Research Start-up Fund for the East China University of Technology (No. DHBK2019060).

Appendix A. Supplementary data

Supplementary data to this article can be found online at https://doi.org/10.1016/j.oregeorev.2021.104598.

References

Chen, G.J., Shu, L.S., Shu, L.M., Zhang, C., Ouyang, Y.P., 2015. Geological characteristics and mineralization setting of the Zhuxi tungsten (copper) polymetallic deposit in the Eastern Jiangnan Orogen. Sci. China: Earth Sci. 45 (12), 1799–1818 (in Chinese with English abstract).

Chen, M.S., Xiang, X.K., Zhan, G.L., Yin, Q.Q., Yu, Z.D., Wang, T.C., Xu, Y.M., Tan, R., 2020. Geochronology, Geochemical Characteristics of the Post-mineralization Late Yanshanian Granite Porphyry and its Constraints for the Terminal of the Metallogeny in the No. 1 Ore Belt of the Dahutang District. Journal of East China University of Technology, 43(05): 401-416 (in Chinese with English abstract).

Chu, P.L., Duan, Z., Liao, S.B., Huang, W.C., Hong, W.T., Zhu, Y.H., Shu, X.J., 2019. Petrogenesis and tectonic significances of Late Mesozoic granitoids in the Dahutang area, Jiangxi Province: constraints from Zircon U-Pb dating, mineral-chemistry, geochemistry and Hf isotope. Acta Geol. Sin. 93 (7), 1687–1707 (in Chinese with English abstract).

Dai, P., Mao, J., Wu, S., Xie, G., Luo, X., 2018. Multiple dating and tectonic setting of the Early Cretaceous Xianglushan W deposit, Jiangxi province, south China. Ore Geol. Rev. 95, 1161–1178.

Deng, X.D., Luo, T., Li, J.W., Hu, Z.C., 2019. Direct dating of hydrothermal tungsten mineralization using in situ wolframite U-Pb chronology by laser ablation ICP-MS. Chem. Geol. 515, 94–104.

Fan, X.K., Mavrogenes, J., Hou, Z.Q., Zhang, Z.Y., Wu, X.Y., Dai, J.L., 2019. Petrogenesis and metallogenic significance of multistage granites in Shimensi tungsten polymetallic deposit, Dahutang giant ore field, South China. Lithos 336–337, 326–344.

Feng, C.Y., Zhang, D.Q., Xiang, X.K., Li, D.X., Qu, H.Y., Liu, J.N., Xiao, Y., 2012. Re–Os isotopic dating of molybdenite from the Dahutang tungsten deposit in northwestern Jiangxi Province and its geological implication. Acta Petrol. Sinica 28 (12), 3858–3868 (in Chinese with English abstract).

Feng, C.Y., Wang, H., Xiang, X.K., Zhang, M.Y., 2018. Late Mesozoic granite-related W-Sn mineralization in the northern Jiangxi region, SE China: a review. J. Geochem. Explor. 195, 31–48.

GSJP (Geological Survey of Jiangxi Province), 2016. The verification report of the Dongping Copper polymetallic ore deposit in Wuning County of Jiangxi Province (in Chinese, unpublished).

Harlaux, M., Romer, R.L., Mercadier, J., Morlot, C., Marignac, C., Cuney, M., 2018. 40 Ma years of hydrothermal W mineralization during the Variscan orogenic evolution of the French Massif Central revealed by U-Pb dating of wolframite. Miner. Deposita 53, 21–51.

Hu, Z., Zhou, L., Liu, Y., Zhao, L., Gao, S., 2011. NIST SRM 610–614 matrix induced unique element fractionation in laser ablation ICP-MS at high spatial resolution analysis. Mineral. Mag. 75, 1060.

Hu, Z.H., Lou, F.S., Li, Y.M., Li, J.M., Wang, X.G., Chen, J.P., Zeng, Q.Q., Wu, S.J., Nie, L. M., Gong, L.X., Wen, L.X., Liu, G.F., Li, Q., Yu, X., 2018. Geochrology, Geochemistry and petrogenesis of ore-related granite in the Dongping Tungsten Deposit in Wuning County Jiangxi Province. Earth Sci. 43 (S1), 243–263 (in Chinese with English abstract).

Huang, L.C., Jiang, S.Y., 2012. Zircon U-Pb geochronology, geochemistry and petrogenesis of the porphyric-like muscovite granite in the Dahutang tungsten deposit Jiangxi Province. Acta Petrol. Sinica 28 (12), 3887–3900 (in Chinese with English abstract).

Huang, L.C., Jiang, S.Y., 2013. Geochronology, geochemistry and petrogenesis of the tungsten-bearing porphyritic granite in the Dahutang tungsten deposit Jiangxi Province. Acta Petrol. Sinica 28, 4323–4335 (in Chinese with English abstract).

Huang, L.C., Jiang, S.Y., 2014. Highly fractionated S-type granites from the giant Dahutang tungsten deposit in Jiangnan Orogen, Southeast China: geochronology, petrogenesis and their relationship with W-mineralization. Lithos 202, 207–226.

Jackson, S., Pearson, J., Griffin, W.N., Belousova, E., 2004. The application of laser ablationinductively coupled plasma-mass spectrometry to in situ U-Pb zircon geochronology. Chem. Geol. 211, 47–69.

Jiang, S.Y., Peng, N.J., Huang, L.C., Xu, Y.M., Zhan, G.L., Dan, X.L., 2015. Geological characteristic and ore genesis of the giant tungsten deposits from the Dahutang oreconcentrated district in northern Jiangxi Province. Acta Petrol.gica Sinica 31 (3), 639–655 (in Chinese with English abstract).

Kong, Z.G., Liang, T., Mao, J.W., Xu, S.F., Xu, H.B., Yan, P.P., Jin, X.Y., 2018. Study on petrogenesis of granodiorite, metallogenic epoch and petrogenetic-metallogenetic setting in the Zhuxiling tungsten polymetallic deposit, southern Anhui Province China. Acta Petrol. Sinica 34 (9), 2632–2656 (in Chinese with English abstract).

Li, Y.M., Li, J.M., 2018. Geochemical characteristics and tectonic dynamic significance of two-mica granite in Dongping Tungsten Mine Area. China Tungsten Ind. 33 (2), 1–9 (in Chinese with English abstract).
Li, B., Zhang, Z.Z., Wu, M.A., Zhou, T.F., Zhao, W.G., Cai, X.B., Di, Q.S., 2015. LA-ICP-MS zircon U-Pb age and molybdenite Re–Os dating of the Dawujian W-Mo polymetallic deposit Ningguo. Geol. Bull. China 34 (2/3), 569–578 (in Chinese with English abstract).
Li, J.M., Li, Y.M., Lou, F.S., Hu, Z.H., Zhong, Q.H., Xie, M.M., Tang, F.L., Sha, M., Yang, X.H., Liu, X.Y., Yi, Y.Q., Hu, W.J., Zhu, Q.M., Nie, L.M., Zhu, C.J., Wen, L.X., Zeng, Q.Q., Huang, J.C., Lei, T.H., Xie, R.F., Gong, L.X., Li, Q., 2016. A "Five-storey" Style quartz vein wolframite deposit in Northern Jiangxi Province: the discovery of the Dongping Wolframite Deposit and its geological significance. Acta Geosci. Sinica 37 (3), 379–384 (in Chinese with English abstract).
Lin, R.H., Yin, Q.Q., Xiang, X.K., Liang, F., Yang, X.F., Wang, T.C., Liu, H.Q., Zhou, W.J., Zhu, B., 2021. Molybdenite Re-Os isotopic age of the Kunshan Mo-W-Cu polymetallic deposit in the Jiangxi Province and its evolution of metallogenic geodynamics. Geol. China 1-16[2021-12-09]. https://kns-cnki-net.webvpn.ecut.edu.cn/kcms/detail/11.1167.p.20200601.1733.016.html.
Liu, Y.S., Gao, S., Hu, Z.C., Gao, C.G., Zong, K.Q., Wang, D.B., 2010a. Continental and oceanic crust recycling-induced melt-peridotite interactions in the Trans-North China Orogen: U-Pb dating, Hf Isotopes and trace elements in zircons from mantle xenoliths. J. Petrol. 51, 537–571.
Liu, Y.S., Hu, Z.C., Zong, K.Q., Gao, C.G., Gao, S., Xu, J., Chen, H.H., 2010b. Reappraisement and refinement of zircon U-Pb isotope and trace element analyses by LA-ICP-MS. Chin. Sci. Bull. 55, 1535–1546.
Ludwig, K.R., 2003. User's manual for Isoplot 3.00, a geochronological toolkit for Microsoft Excel. Berkeley Geochronology Center Special Publication No. 4. Components, p. 70.
Luo, L., Jiang, S.Y., Yang, S.Y., Zhao, K.D., Wang, S.L., Gao, W.L., 2010. Petrochemistry, zircon U-Pb dating and Hf isotopic composition of the granitic pluton in the Pengshan Sn–polymetallic orefield, Jiangxi province. Acta Petrol. Sinica 26, 2818–2834 (in Chinese with English abstract).
Mao, Z.H., Cheng, Y.B., Liu, J.J., Yuan, S.D., Wu, S.H., Xiang, X.K., Luo, X.H., 2013. Geology and molybdenite Re–Os age of the Dahutang granite-related veinlets–disseminated tungsten ore field in the Jiangxi Province, China. Ore Geol. Rev. 53, 422–433.
Mao, Z.H., Liu, J.J., Mao, J.W., Deng, J., Zhang, F., Meng, X.Y., Kang, X.B., Xiang, X.K., Luo, X.H., 2015. Geochronology and geochemistry of granitoids related to the giant Dahutang tungsten deposit, middle Yangtze River region, China: implications for petrogenesis, geodynamic setting, and mineralization. Gondwana Res. 28 (2), 816–836.
Mao, J.W., Wu, S.H., Song, S.W., Dai, P., Xie, G.Q., Su, Q.W., Liu, P., Wang, X.G., Yu, Z. Z., Chen, X.Y., Tang, W.X., 2020. The world-class Jiangnan tungsten belt: Geological characteristics, metallogeny, and ore deposit model. Chin. Sci. Bull. 65 (33), 3746–3762 (in Chinese with English abstract).
Mao, J.W., Xiong, B.K., Liu, J., Pirajno, F., Cheng, Y.B., Ye, H.S., Song, S.W., Dai, P., 2017. Molybdenite Re–Os dating, zircon U-Pb age and geochemistry of granitoids in the Yangchuling porphyry W–Mo deposit (Jiangnan tungsten ore belt), China: implications for petrogenesis, mineralization and geodynamic setting. Lithos 286, 35–52.
Mao, J.W., Ouyang, H.G., Song, S.W., Santosh, M., Yuan, S.D., Zhou, Z.H., Zheng, W., Liu, H., Liu, P., Chen, Y.B., Chen, M.H., 2019. Geology and Metallogeny of Tungsten and Tin Deposits in China: Society of Economic Geologists Special. Publication 22, 411–482.
Pan, X.F., Hou, Z.Q., Li, Y., Chen, G.H., Zhao, M., Zhang, T.F., Zhang, C., Wei, J., Kang, C., 2017. Dating the giant Zhuxi W-Cu deposit (Taqian–Fuchun Ore Belt) in South China using molybdenite Re–Os and muscovite Ar–Ar system. Ore Geol. Rev. 86, 719–733.
Peng, N.J., Jiang, S.Y., Xiong, S.F., Pi, D.H., 2018. Fluid evolution and ore genesis of the Dalingshang deposit, Dahutang W-Cu ore field, northern Jiangxi Province, South China. Miner. Deposita 53, 1079–1094.
Qin, Y., Wang, D.H., Wu, L.B., Wang, K.Y., Mei, Y.P., 2010. Zircon SHRIMP U-Pb Dating of the Mineralized Porphyry in the Dongyuan W Deposit in Anhui Province and its Geological Significance. Acta Geol. Sin. 84 (4), 479–484.
Song, W.L., Yao, J.M., Chen, H.Y., Sun, W.D., Lai, C.k., Xiang, X.K., Luo, X.H., Jourdan, F, 2018. A 20 m.y. long-lived successive mineralization in the giant Dahutang W–Cu–Mo deposit, South China. Ore Geol. Rev., 95, 401–407.
Song, G.X., Qin, K.Z., Li, G.M., Li, X.H., Qu, W.J., 2012. Geochronology and ore-forming fluids of the Baizhangyan W-Mo deposit in the Chizhou Area, middle-lower Yangtze Valley SE-China. Resour. Geol. 63 (1), 57–71.
Song, G.X., Qin, K.Z., Li, G.M., Liu, T.B., Li, J.X., Li, X.H., Chang, Z.S., 2012. Geochronologic and isotope geochemical constraints on magmatism and associated W-Mo mineralization of the Jitoushan W–Mo deposit, middle–lower Yangtze Valley. Int. Geol. Rev. 54 (13), 1532–1547.
Su, Q.W., Mao, J.W., Wu, S.H., Zhang, Z.C., Xu, S.F., 2018. Geochronology and geochemistry of the granitoids and ore–forming age in the Xiaoyao tungsten polymetallic skarn deposit in the Jiangnan Massif tungsten belt, China: Implications for their petrogenesis, geodynamic setting, and mineralization. Lithos 296–299, 365–381.
Tang, Y.W., Cui, K., Zheng, Z., Gao, J.F., Han, J.J., Yang, J.H., Liu, L., 2020. LA-ICP-MS U-Pb geochronology of wolframite by combining NIST series and common lead-bearing MTM as the primary reference material: Implications for metallogenesis of South China. Gondwana Res. 83, 217–231.
Tang, Y.W., Gao, J.F., Lan, T.G., Cui, K., Han, J.J., Zhang, X., Chen, Y.W., Chen, Y.H., 2021. In situ low-U garnet U-Pb dating by LA-SF-ICP-MS and its application in constraining the origin of Anji skarn system combined with Ar-Ar dating and Pb isotopes. Ore Geol. Rev. 130, 103970.
Tang, C., Yang, X.Y., Cao, J.Y., 2019. Genesis of the Shangjinshan W-Mo polymetallic deposit in the Eastern Jiangnan tungsten belt: evidences from geochemistry, geochronology and zircon Hf isotope analyses. Ore Geol. Rev. 115.
Vermeesch, P., 2012. On the visualisation of detrital age distributions. Chem. Geol. 312–313, 190–194.
Wang, H., Feng, C.Y., Li, D.X., Xiang, X.K., Zhou, J.H., 2015. Sources of granitoids and ore-forming materials of Dahutang tungsten deposit in northern Jiangxi Province: constrains from mineralogy and isotopic tracing. Acta Pet. Sin. 31 (3), 725–739 (in Chinese with English abstract).
Wei, W.F., Yan, B., Shen, N.P., Liu, L., Zhang, Y., Xiang, X.K., 2017. Muscovite 40Ar/39Ar age and H-O-S isotopes of the Shimensi Tungsten Deposit (Northern Jiangxi Province, South China) and their Metallogenic Implications. Minerals 7, 162.
Wilde, S.A., Valley, J.W., Peck, W.H., Graham, C.M., 2001. Evidence from detrital zircons for the existence of continental crust and oceans on the Earth 4.4 Gyr ago. Nature 409, 175–178.
Wu, S.H., Mao, J.W., Yu, H., Tan, D.R., Geng, X.X., 2021. Upper temperature limits of orogenic gold deposit formation: constraints from TiO_2 polymorphs in the Dongyuan Au deposit, Jiangnan Orogen, China. Am. Mineral. 106, 1809–1817.
Wu, S.H., Sun, W.D., Wang, X.D., 2019a. A new model for porphyry W mineralization in a world-class tungsten metallogenic belt. Ore Geol. Rev. 107, 501–512.
Wu, S.H., Mao, J.W., Trevor, R., Zhao, Z., Yao, F.J., Yang, Y.P., 2019b. Comparative geochemical study of scheelite from the Shizhuyuan and Xianglushan tungsten skarn deposits, South China: implications for scheelite mineralization. Ore Geol. Rev., 109, 448–464.
Xiao, X., Zhou, T.F., Yuan, F., Fan, Y., Zhang, D.Y., Liu, D.Z., Huang, W.P., Chen, X.F., 2017. The geochronology of the Qingyang Gaojiabang tungsten-molybdenum deposit and its geological significance, Anhui Province East China. Acta Petrol. Sinica 33 (3), 859–872 (in Chinese with English abstract).
Xiang, X.K., Wang, P., Zhan, G.N., Sun, D.M., Zhong, B., Qian, Z.Y., Tan, R., 2013a. Geological characteristics of Shimensi tungsten polymetallic deposit in northern Jiangxi Province. Mineral Deposits 32 (6), 1171–1187 (in Chinese with English abstract).
Xiang, X.K., Wang, P., Sun, D.M., Zhong, B., 2013b. Re–Os isotopic age of molybdeinte from the Shimensi tungsten polymetallic deposit in northern Jiangxi province and its geological implications. Geol. Bull. China 32 (11), 1824–1831 (in Chinese with English abstract).
Xu, B., Jiang, S.Y., Luo, L., 2015. LA–MC–ICP–MS U-Pb dating of cassiterite from the Jianfengpo Sn deposit in the Pengshan Sn–polymetallic ore field, Jiangxi Province and its geological significance. Acta Petrol. Sinica 31 (3), 701–708 (in Chinese with English abstract).
Xu, D.R., Zou, F.H., Ning, J.T., Deng, T., Wang, Z.L., Chen, G.W., Zhang, J.L., Dong, G.J., 2017. Discussion on geological and structural characteristics and associated metallogeny in northeastern Hunan province South china. Acta Petrol. Sinica 33 (3), 695–715 (in Chinese with English abstract).
Yan, C., Chen, Z.H., Yang, L.Q., Wang, Y.Q., Zeng, L., Hu, Z.K., 2017. U-Pb Dating of Mineralization Rock Zircon in Dongping Copper Tungsten Mine and Its Geological Significance. China Tungsten Ind. 32 (3), 1–11 (in Chinese with English abstract).
Yang, M., Yang, Y.H., Wu, S.T., Romer, R.L., Che, X.D., Zhao, Z.F., Li, W.S., Yang, J.H., Wu, F.Y., Xie, L.W., Huang, C., Zhang, D., Zhang, Y., 2020a. Accurate and precise in situ U-Pb isotope dating of wolframite series minerals via LA-SF-ICP-MS. J. Anal. At. Spectrom. 35, 2191–2203. https://doi.org/10.1039/D0JA00248H.
Yang, S.W., Lou, F.S., Ding, P.X., Zhang, F.R., 2020b. Mesozoic Magmatism and Tungsten Mineralization in Northern Jiangxi. China Tungsten Ind. 35 (5), 53–60 (in Chinese with English abstract).
Ye, H.M., Zhang, X., Zhu, Y.H., 2016. In-situ monazite U-Pb geochronology of granites in Shimensi tungsten polymetallic deposit, Jiangxi province and its geological significance. Geotect. Metal. 40, 58–70 (in Chinese with English abstract).
Yu, Z.D., Xiang, X.K., Tan, R., Sun, D.M., Zhang, X., 2020. Zircon U-Pb chronology, geochemistry and geological significance of coarse muscovite granite in Pingmiao Mining Area of Dahutang North Jiangxi. J. Jilin Univ. (Earth Sci. Ed.) 50 (5), 1505–1517 (in Chinese with English abstract).
Zhao, C., Xie, X.N., Ma, C., Liu, J.X., Chao, C.H., 2015. Geological significance of zircon age and Re–Os isotopic measurement on molybdenite from Matou Cu-Mo polymetallic deposit Chizhou, Anhui Province, China. Chinese J. Nonferrous Metals 25 (12), 3461–3472 (in Chinese with English abstract).
Zhang, Z.H., Geng, L., Jia, W.B., Gong, X.D., Du, Z.Z., Zhang, M.C., 2014. Regional geological characteristics study of tungsten-polymetallic ore field in Datanghu tungsten polymetallic deposit in north of Jiangxi Chin. Min. Maga. 23, 133–148 (in Chinese with English abstract).
Zhang, M.Y., Feng, C.Y., Li, D.X., Wang, H., Zhou, J.H., Ye, S.Z., Wang, G.H., 2016. Geochronological study of the Kunshan W-Mo–Cu deposit in the Dahutang area,

northern Jiangxi province and its geological significance. Geotect. Metal. 40, 503–516 (in Chinese with English abstract).
Zhang, Z.H., Zhang, D., Wu, G.G., Luo, P., Chen, X.H., Di, Y.J., Lü, L.J., 2013. Re–Os isopotic age of molybdenite from the Meizikeng molybdenite deposit in Northern Jiangxi Province and Its Geological Significance. J. Jilin Univ. (Earth Sci. Edition) 43 (6), 1851–1863 (in Chinese with English abstract).
Zhang, J.J., Mei, Y.P., Wang, D.H., Li, H.Q., 2008. Isochronology study on the Xianglushan Scheelite deposit in North Jiangxi Province and its geological significance. Acta Geosci. Sinica 82 (7), 927–931 (in Chinese with English abstract).
Zhang, Y., Pan, J.Y., Ma, D.S., Dan, X.H., Zhang, L.L., Xu, G.H., Yang, C.P., Jiang, Q.X., Jiang, C.Q., 2017. Re–Os molybdenite age of Dawutang tungsten ore district of northwest Jiangxi and its geological significance. Mineral Deposits 36 (3), 749–769 (in Chinese with English abstract).
Zhong, Y.F., Ma, C.Q., She, Z.B., Lin, G.C., Xu, H.J., Wang, R.J., Yang, K.G., Liu, Q., 2005. SHRIMP U-Pb Zircon Geochronology of the Jiuling Granitic Complex Batholith in Jiangxi Province. Earth Sci.-J. China Univ. Geosci. 30 (6), 685–691 (in Chinese with English abstract).
Zhou, X., Yu, X.Q., Wang, D.E., Zhang, D.H., Li, C.L., Fu, J.Z., Dong, H.M., 2011. Characteristics and geochronology of the W, Mo-bearing Granodiorite Porphyry in Dongyuan SouthernAnhui. Geoscience 25 (2), 201–210 (in Chinese with English abstract).